Proceedings of the 17th World Congress
The International Federation of Automatic Control
Seoul, Korea, July 6-11, 2008

Modeling and Straight Transfer Transformation Control of Shipboard Crane Considering Ship Sway

Ryuji Ito * **Kazuya Hieda** * **Kazuhiko Terashima** *
Akihiro Kaneshige **

* *Dept. of Production Systems Engineering, Toyohashi University of Technology, Hibarigaoka 1-1, Tempaku-cho, Toyohashi, 441-8580 Japan*
E-mail: ({ito, hieda, terasima}@syscon.pse.tut.ac.jp)
** *Dept. of Mechanical Engineering, Toyota National College of Technology, Aisei-cho 2-1, Toyota, 471-8525 Japan*
E-mail: (kanesige@toyota-ct.ac.jp)

Abstract: The purpose of this paper was to develop a control system for a shipboard crane that considers safety and work efficiency. A shipboard crane model was built and a straight-transfer transformation control system was designed. In order to realize transfer trajectory control, a Two-Degree-of-Freedom (2-DOF) control system was applied. It was demonstrated that the work efficiency of transferring a load to a target position can be improved by considering shipboard sway, by using a 2-DOF system that combines a feedforward control system with a feedback control system, and making the transfer trajectory follow the desired one.

1. INTRODUCTION

Rotary cranes transfer loads by three motions: rotation, luffing, and load hoisting. Cranes are widely used on construction sites and at factories and ports, because they can transfer a heavy load, its structure is simple, and the equipment can be assembled on the spot. However, there are still many issues in the performance of rotary cranes, such as load sway, positioning, obstacle avoidance, and so on. Moreover, in the shipboard cranes, which transfer loads using a rotary crane attached to the ship's deck as shown in Fig. 1, the operator has to deal with the sway of the ship as the crane transfers cargo. The influence of the ship sway with a rotary crane makes the problems mentioned above still more difficult. Shipboard sway is generated by disturbances such as waves and winds, as well as movements of the load. Up to the present, these problems have been solved by the experience and intuition of expert operators with high skill levels. This is extremely difficult and intense work, since the operator must execute the tasks while considering both work efficiency and safety.

Numerous researches on rotary crane have been reported (see Shen et al.[2003] and Terashima et al.[2007]). The authors have proposed the Straight Transfer Transformation (STT) method by transferring a load along a straight path using simultaneous movements of rotation, luffing and hoisting, to avoid exaggerated swaying of the load owing to the centrifugal force caused by rotation (see Shen et al.[2003] and Terashima et al.[2007]). With respect to shipboard cranes, there are fewer researches, although shipboard crane control is important. When the crane weight is very small in relation to the ship weight, special care is not required. Nonetheless, ship (hull) sway requires special attention to realize a reasonable control design. Research on shipboard cranes with respect to three-dimensional

Fig. 1. A shipboard crane

motion and sway control of both ship and crane's load has been lacking (see Todd et al.[1997], Wen et al.[1999], Kimiaghalam et al.[1999], Chin et al.[1998], and Tsutsui et al.[2006]). If conventional control is applied in a case in which ship sway is non-negligible, the transfer of the load to the target position cannot be achieved. Therefore, in this research, the STT method is applied to the case of a shipboard crane to avoid the influence of centrifugal force. Then, the position and sway control of a load is studied, considering the ship's sway generated by the crane motion.

This paper presents a transfer control that addresses the influence of crane motion on ship sway in a cargo ship system using a shipboard crane. First, in order to analyze the motions of a shipboard crane, a model of a shipboard crane is designed, and then the transfer control system is designed for it. The shipboard crane model is a mathematical model combining a rotary crane model and a shipboard sway model. The transfer trajectory control employs a two-degree-of-freedom (2-DOF) control system. The 2-DOF control system is constituted by a feedforward control using Straight Transfer Transformation (STT) and a notch filter, and a feedback control using an optimal

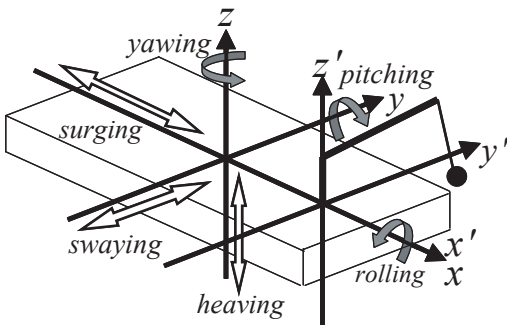

Fig. 2. Schematic diagram of a shipboard crane

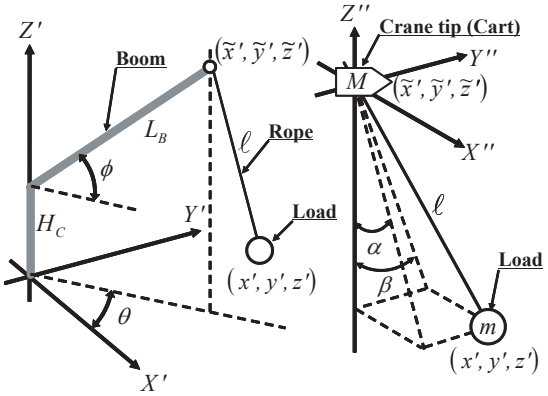

Fig. 3. Schematic diagram of a rotary crane for the swing angle model

servo control. As a result, a high-speed transfer system controlling the sway of the ship by feedforward control was achieved, and the deviation between the output trajectory and reference was compensated by feedback control.

The proposed method was confirmed by the simulation analysis to be effective at reducing ship sway and load sway due to the 2-DOF control system.

2. MODELING OF SHIPBOARD CRANE

The mathematical model of the shipboard crane in this paper was comprised of two parts: the rotary crane and the sway of the ship to which it is attached. A schematic diagram of the shipboard crane is shown in Fig. 2, in which the form of the ship is represented by a rectangular parallelepiped, the absolute coordinate system $\sum$ is an $X-Y-Z$ coordinate system fixed in space, and the crane coordinate system $\sum'$ is an $X'-Y'-Z'$ coordinate system fixed to the rotary crane.

2.1 Crane model

In order to derive the crane model, the swing angle of the load was observed. A schematic diagram of the rotary crane is shown in Fig. 3, and the parameters in Fig. 3 are shown in Table 1, where α[rad] is the load swing angle of the X-direction, β[rad] is the load swing angle of the Y-direction, $(\tilde{x}, \tilde{y}, \tilde{z})$[m] is the boom tip position, (x, y, z)[m] is the load position, θ[rad] is the rotary angle, and ϕ[rad] is the boom hoisting angle.

A boom tip is assumed to be a cart which moves, and

Table 1. Parameters of the crane model

symbol	unit	appellation	value
L_B	m	length of the boom	19
H_c	m	height of the turn table	1.5
l	m	length of the rope	15
m	ton	mass of the load	240
g	m/s^2	gravity acceleration	9.81

Eqs.(1) and (2) are respectively obtained by the Lagrange equation of motion.

$$\ddot{\alpha} = f_1\left(\dddot{\tilde{x}}, \dddot{\tilde{y}}, \dddot{\tilde{z}}, \dot{\alpha}, \alpha, \dot{\beta}, \beta\right) \tag{1}$$

$$\ddot{\beta} = f_2\left(\dddot{\tilde{x}}, \dddot{\tilde{y}}, \dddot{\tilde{z}}, \dot{\alpha}, \alpha, \dot{\beta}, \beta\right) \tag{2}$$

Eqs.(1) and (2) for the crane model are respectively described in Appendix A.

2.2 Ship sway model

Generally, a ship performs six degree-of-freedom motion as shown in Fig. 3. However, while shipping and discharging the load by transfer work using a shipboard crane, the heaving motion by change of the load weight becomes as important as any rolling and pitching motion. It is assumed that the surging, swaying and a yawing motion generated from the transfer of the rotary crane is small. Thus, the mathematical model of the ship sway took into consideration rolling, heaving and pitching among the six degree of freedom motion. The mathematical model of ship sway is as follows, and the parameters used by the ship sway model are shown in Table 2. The mathematical model of ship sway introduces the torque of the load at the boom tip position as the external force which causes the ship's inclination and sway.

$$I\frac{d^2\rho_x}{dt^2} + M_S \cdot g \cdot \overline{GM}\rho_x = F_y = mg\tilde{y} \tag{3}$$

$$I_l\frac{d^2\rho_y}{dt^2} + M_S \cdot g \cdot \overline{GM_l}\rho_y = F_y = mg\tilde{x} \tag{4}$$

$$M_S g\frac{d^2\delta}{dt^2} + \rho g A_w \delta = F_z = m\left(g + \ddot{z}\right), \tag{5}$$

where ρ_x[rad] is the inclination angle of the ship in the X-direction, ρ_y[rad] is inclination angle of the ship in the Y-direction, and δ[m] is the displacement of the ship in the Z-direction.

Table 2. Parameters of the ship sway model

symbol	unit	appellation	value
M_S	ton	mass of the ship	2400
L_S	m	length of the shipboard	30
B_S	m	width of the shipboard	13
H_S	m	height of the shipboard	2.5
D_l	m	distance from center of the ship to the crane	2.5
A_w	m^2	area of water plane of the ship	390
I	kN·m^2	inertia moment of X-direction	6615.3
I_l	kN·m^2	inertia moment of Y-direction	35229
$\overline{GM}$	m	transverse metacenter height	8.89
$\overline{GM_l}$	m	longitudinal metacenter height	49.5
ρ	kg/m^3	density of seawater	1.025

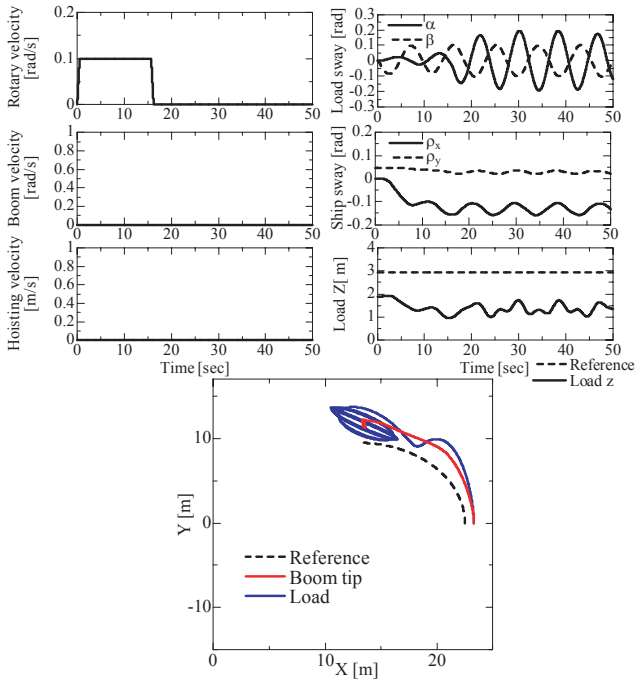

Fig. 4. Simulation results of rotary transfer

2.3 Shipboard crane model

As mentioned above, the crane model and the ship sway model were obtained. Here, the crane model indicates the sway of the load, and the ship sway model indicates the sway of the ship. The shipboard crane model is derived by combining these two models. Since the parameters of the crane model are expressed by the crane coordinate system, these are converted into the absolute coordinate system. Then, in consideration of the ship inclination and ship sway, the coordinates for the boom tip position are transformed from the crane coordinate system to the absolute coordinate system. As a result, the boom tip position expressed by the absolute coordinate system is shown as follows:

$$\ddot{\tilde{x}} = f_3\left(\ddot{\rho_x}, \ddot{\rho_y}, \dot{\rho_x}, \dot{\rho_y}, \rho_x, \rho_y, \ddot{\theta}, \dot{\theta}, \theta, \ddot{\phi}, \dot{\phi}, \phi\right) \quad (6)$$

$$\ddot{\tilde{y}} = f_4\left(\ddot{\rho_x}, \ddot{\rho_y}, \dot{\rho_x}, \dot{\rho_y}, \rho_x, \rho_y, \ddot{\theta}, \dot{\theta}, \theta, \ddot{\phi}, \dot{\phi}, \phi\right) \quad (7)$$

$$\ddot{\tilde{z}} = f_5\left(\ddot{\rho_x}, \ddot{\rho_y}, \dot{\rho_x}, \dot{\rho_y}, \rho_x, \rho_y, \ddot{\phi}, \dot{\phi}, \phi, \ddot{\delta}, \dot{\delta}, \delta\right) \quad (8)$$

The swing angle of the load can be found by substituting the boom tip position of Eqs.(A.14) and (A.15) into Eqs.(6)∼(8). This is the shipboard crane model.

Eqs.(6)∼(8) for a crane model are described in Appendix B.

3. ANALYSIS OF THE SHIPBOARD CRANE MODEL

In order to clarify the validity of the shipboard crane model and the transfer characteristics in a shipboard crane, a simulation by rotational transfer, which is the basic motion of a rotary crane, was performed, and the result is shown in Fig. 4, where *Reference* shows the transfer trajectory in the case in which the ship does not incline.

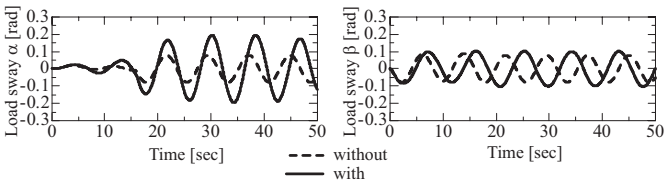

Fig. 5. Comparison by simulation between the shipboard crane with and without ship's sway

In the X-Y plane of Fig. 4, it is confirmed that the transfer trajectory under the influence of centrifugal force and the inclination of the ship falls outside the *Reference* trajectory. After the end of conveyance, since a load sways greatly under the influence of transfer acceleration and centrifugal force and the ship is also swayed, it turns out that the boom tip position changes. Moreover, the swing angle of the rotary crane using the same input and the shipboard crane model are shown in Fig. 5.

From Fig. 5, load transfer by shipboard crane considering ship sway has a large sway amplitude compared with the case without ship sway, and it is confirmed that the oscillating cycle of the rotary crane differs in the two cases. Through these simulation results concerning ship and load sway, the obtained motion is thought to be reasonable. Therefore, the control design is derived using this model. Model validity must be checked in the near future by experiments and Fluid Computational Simulation (Commercial software: Flow-3D), which is being planned now by the authors. By the way, in experiments, rotary angle, boom luffing angle and rope length are measured by encoders, and the swing angle of the rope is measured by a laser sensor. The inclination angle of the ship is measured by a gyroscope sensor.

4. TWO-DEGREE-OF-FREEDOM CONTROL SYSTEM

Load sway and ship sway, and transfer trajectory control in consideration of the inclination of a ship can be studied by the proposed shipboard crane model. The transfer control system was built by a 2-DOF control system shown in Fig. 6, where the *FFcontroller* is the controller that produces the sway suppression control input from the straight transfer reference p of the load position instructions. On the other hand, *FBcontroller* is the controller that produces the control input u_{FF} to compensate for the error between the target transfer trajectory $p_d = (\tilde{x}_d,\ \tilde{y}_d,\ \tilde{z}_d,\ x_d,\ y_d,\ z_d)$ and the actual transfer trajectory $(\tilde{x},\ \tilde{y},\ \tilde{z},\ x,\ y,\ z)$. The *STTconverter* is the converter that transforms the control input generated on the straight transfer trajectory into the rotary input, the boom luffing input and the rope hoisting input. *Converter*1 is a converter that computes the transfer trajectory reference p_d from the initial condition of the ship and the straight transfer input u_{FF}. *Converter*2 is a converter that computes the actual boom tip position $(\tilde{x},\ \tilde{y},\ \tilde{z})$ and load position $(x,\ y,\ z)$ from the actual output $(\theta,\ \phi,\ l,\ \alpha,\ \beta,\ \rho_x,\ \rho_y)$ of a plant. *Converter*3 is a converter that transforms the output of $\ddot{\tilde{x}}_e,\ \ddot{\tilde{y}}_e,\ \ddot{\tilde{z}}_e$ from a feedback controller into the rotary crane input of $\dot{\theta},\ \dot{\phi},\ \dot{l}$.

This system has structures for sway suppression control

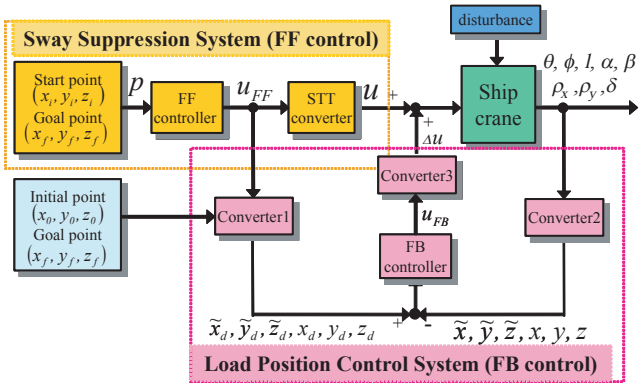

Fig. 6. Block diagram of the 2-degree-of-freedom system

without disturbances such as ship inclination, ship sway, and wind, performed by the feedforward controller part (FF), and for tracking control with the target trajectory against disturbances, performed by the feedback controller part (FB). Then, the load's sway suppression transfer can be performed while following the target trajectory by the proposed transfer control system.

4.1 Design of a feedforward controller

For the Sway Suppression System (FF control), which performs the transfer to a target position, the STT method was adopted to remove the centrifugal force component. Thereby, in this model, the load can be considered as a single pendulum model which moves in a straight line to the target position, and performs sway suppression control. As the sway suppression control, a nonlinear optimal control can be performed, as in Terashima's paper (Terashima et al.[2007]). However, since this algorithm was rather complicated, the Frequency Shape Approach (FSA) method was used with little computational effort, where FSA is the method of removing the natural frequency of the controlled object from the frequency of an input by notch filter. The controlled objects were the load and the ship. Since the natural frequency of the load is determined by the rope length, robustness is secured with a triple-notch filter, or the multiplication of three notch filters, which suppresses the sway of the load. The sway of the ship is suppressed using the double-notch filter in consideration of the natural frequency of pitching and rolling. Therefore, a quintuple-notch filter, or the product of the triple-notch filter for sway suppression control of a load multiplied by the double-notch filter for ship sway suppression control, was applied for the control system.

The transfer function of each notch filter is shown in Eq.(9).

$$K_{N,i}(s) = \frac{s^2 + 2\zeta_N \omega_{N,i} s + \omega_{N,i}^2}{s^2 + \omega_{N,i} s + \omega_{N,i}^2} \quad (i = 1, 2, \cdots, 5) \quad (9)$$

Moreover, the feedforward controller was given as Eq.(10) in consideration of noise and the response to the transfer reference input.

$$K(s) = \frac{N(s)}{D(s)_1 + D(s)_2}, \quad (10)$$

where

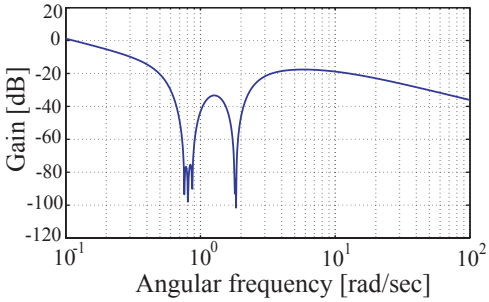

Fig. 7. Gain diagram of the proposed controller

$$N(s) = (K_P s + K_I) \prod_{i=1}^{5} (s^2 + 2\zeta_N \omega_{N,i} s + \omega_{N,i}^2) \quad (11)$$

$$D(s)_1 = s(T_L s + 1) \prod_{i=1}^{5} (s^2 + \omega_{N,i} s + \omega_{N,i}^2) \quad (12)$$

$$D(s)_2 = (K_P s + K_I) \prod_{i=1}^{5} (s^2 + 2\zeta_N \omega_{N,i} s + \omega_{N,i}^2) \quad (13)$$

Here, K_P, K_I and T_L of Eq.(10) are unknown parameters (see Yano et al.[2001]). The unknown parameters were decided by the optimization method using the simplex method. The gain diagram of the proposed feedforward controller is shown in Fig. 7, and the natural frequencies of the quintuple-notch-filter are shown in Table 3. Then, K_P=0.220, K_I=0.123 and K_D=0.173.

Table 3. Frequency of notch filter

	$\omega_{N,1}$	$\omega_{N,2}$	$\omega_{N,3}$
Rope length [m]	13	15	17
Frequency [rad/s]	0.8687	0.8087	0.7596

	$\omega_{N,4}$	$\omega_{N,5}$
Ship sway direction	X-direction	Y-direction
Frequency[rad/s]	1.7959	1.8364

4.2 Design of a feedback controller

Derivation of linear position error model of a rotary crane : In order to obtain feedback gain, the position error model is derived by state variables of the load position error and the boom tip error. In load transfer by rotary crane, the boom tip position in the target trajectory is represented by $(\tilde{x}_d, \tilde{y}_d, \tilde{z}_d)$, the load position by (x_d, y_d, z_d), the boom tip position in the actual transfer trajectory by $(\tilde{x}, \tilde{y}, \tilde{z})$, and the load position by (x, y, z). Then the error of the position can be defined as follows:

$$\tilde{x}_e = \tilde{x} - \tilde{x}_d, \quad \tilde{y}_e = \tilde{y} - \tilde{y}_d, \quad \tilde{z}_e = \tilde{z} - \tilde{z}_d \quad (14)$$

$$x_e = x - x_d, \quad y_e = y - y_d, \quad z_e = z - z_d \quad (15)$$

Differentiating the above formulas two times, the following formulas can be obtained:

$$\ddot{\tilde{x}}_e = \ddot{\tilde{x}} - \ddot{\tilde{x}}_d = u_x - u_{xd} = u_{ex} \quad (16)$$

$$\ddot{\tilde{y}}_e = \ddot{\tilde{y}} - \ddot{\tilde{y}}_d = u_y - u_{yd} = u_{ey} \quad (17)$$

$$\ddot{\tilde{z}}_e = \ddot{\tilde{z}} - \ddot{\tilde{z}}_d \quad (18)$$

$$\ddot{x}_e = \frac{x-\tilde{x}}{z-\tilde{z}}(\ddot{z}+g) - \frac{x_d-\tilde{x}_d}{z_d-\tilde{z}_d}(\ddot{z}_d+g) \quad (19)$$

$$\ddot{y}_e = \frac{y-\tilde{y}}{z-\tilde{z}}(\ddot{z}+g) - \frac{y_d-\tilde{y}_d}{z_d-\tilde{z}_d}(\ddot{z}_d+g) \quad (20)$$

$$\ddot{z}_e = \ddot{z} - \ddot{z}_d \ , \quad (21)$$

where

$$\ddot{\tilde{z}} = -\frac{u_x\tilde{x}+u_y\tilde{y}+\dot{\tilde{x}}^2+\dot{\tilde{y}}^2}{\tilde{z}-H_C} + \frac{\dot{\tilde{x}}\tilde{x}+\dot{\tilde{y}}\tilde{y}}{(\tilde{z}-H_C)^2}\dot{\tilde{z}} \quad (22)$$

$$\ddot{\tilde{z}}_d = -\frac{u_{xd}\tilde{x}_d+u_{yd}\tilde{y}_d+\dot{\tilde{x}}_d^2+\dot{\tilde{y}}_d^2}{\tilde{z}_d-H_C} + \frac{\dot{\tilde{x}}_d\tilde{x}_d+\dot{\tilde{y}}_d\tilde{y}_d}{(\tilde{z}_d-H_C)^2}\dot{\tilde{z}}_d \quad (23)$$

$$\ddot{z} = \frac{e_z^2}{l^2}(\ddot{\tilde{z}} + \frac{u_xe_x+u_ye_y-\dot{e}_x^2-\dot{e}_y^2-\dot{e}_z^2}{e_z} - \frac{e_x^2+e_y^2}{e_z^2}g) \quad (24)$$

$$\ddot{z}_d = \frac{e_{zd}^2}{l^2}(\ddot{\tilde{z}}_d + \frac{u_{xd}e_{xd}+u_{yd}e_{yd}-\dot{e}_{xd}^2-\dot{e}_{yd}^2-\dot{e}_{zd}^2}{e_{zd}} - \frac{e_{xd}^2+e_{yd}^2}{e_{zd}^2}g) \quad (25)$$

$$e_x = x-\tilde{x}, \quad e_y = y-\tilde{y}, \quad e_z = z-\tilde{z} \quad (26)$$

$$e_{xd} = x_d-\tilde{x}_d, \quad e_{yd} = y_d-\tilde{y}_d, \quad e_{zd} = z_d-\tilde{z}_d \quad (27)$$

The nonlinear position error model of the rotary crane was described in the above formula. In order to easily build the feedback controller, the nonlinear position error model is linearized. In a rotary crane, if the rope length is constant and the swing angle is minute, the changing of the load position in the Z-direction is very small. As a result, the approximate expression of Eq.(28) is obtained.

$$z-\tilde{z} = l, \quad \ddot{\tilde{z}} = 0, \quad z_d-\tilde{z}_d = l, \quad \ddot{\tilde{z}}_d = 0 \quad (28)$$

When Eq.(28) is applied to the nonlinear position error model of Eqs.(16)$\sim$(21), it follows that

$$\ddot{\tilde{x}}_e = u_{ex} \ , \quad \ddot{\tilde{y}}_e = u_{ey} \quad (29)$$

$$\ddot{x}_e = -\frac{x_e-\tilde{x}_e}{l}g \ , \quad \ddot{y}_e = -\frac{y_e-\tilde{y}_e}{l}g \quad (30)$$

The linear position error model is shown in the above formulas, and can be written as follows:

$$\dot{X}_{ex} = AX_{ex}+Bu_{ex} \ , \ Y_{ex} = [\tilde{x}_e, \ x_e]^T = CX_{ex} \quad (31)$$

$$\dot{X}_{ey} = AX_{ey}+Bu_{ey} \ , \ Y_{ey} = [\tilde{y}_e, \ y_e]^T = CX_{ey} \ , \quad (32)$$

where

$$X_{ex} = \left[\tilde{x}_e, \ \dot{\tilde{x}}_e, \ x_e, \ \dot{x}_e\right]^T \ , \quad X_{ey} = \left[\tilde{y}_e, \ \dot{\tilde{y}}_e, \ y_e, \ \dot{y}_e\right]^T$$

$$A = \begin{bmatrix} 0 & 1 & 0 & 0 \\ 0 & 0 & 0 & 0 \\ 0 & 0 & 0 & 1 \\ \frac{g}{l} & 0 & -\frac{g}{l} & 0 \end{bmatrix}, \quad B = \begin{bmatrix} 0 \\ 1 \\ 0 \\ 0 \end{bmatrix},$$

$$C = [\,1 \ 0 \ 1 \ 0\,]$$

The linear position error model of the rotary crane has been shown in the above formula.

Calculation of a feedback controller gain : The feedback controllers of the X-direction and Y-direction by the optimal servo system are built by using the obtained linear position error model. Feedback controller gain is reasonably computed by using the optimal regulator design method. In order to solve the control problem such that the output value coincides with the desired value, an extended system is built as follows:

$$\frac{d}{dt}\begin{bmatrix} \dot{X}_{ei} \\ e_i \end{bmatrix} = \begin{bmatrix} A & 0 \\ -C & 0 \end{bmatrix}\begin{bmatrix} \dot{X}_{ei} \\ e_i \end{bmatrix} + \begin{bmatrix} B \\ 0 \end{bmatrix}\dot{u}_{ei} \ , \quad (33)$$

where the error is defined by

$$e_{id} = r_{ei}(t) - y_{ei}(t) \ , \quad (i = x, y) \quad (34)$$

In order to obtain feedback gain, the cost function of Eq.(35) is given.

$$J = \int_0^\infty \left\{ \begin{bmatrix} \dot{X}_{ei} \\ e_{id} \end{bmatrix}^T Q \begin{bmatrix} \dot{X}_{ei} \\ e_{id} \end{bmatrix} + R\dot{u}_{ei}^2 \right\} \quad (35)$$

$$Q = [\,q_1 \ q_2 \ q_3 \ q_4 \ q_5\,], \quad R = 1 \ ,$$

where Q and R are the weighting matrix of the cost function. If the extended system is a controllable system, the state feedback is shown as follows:

$$\dot{u}_{ei} = -R^{-1}\begin{bmatrix} B \\ 0 \end{bmatrix}^T S \begin{bmatrix} \dot{X}_{ei} \\ e_{id} \end{bmatrix} \ , \quad (36)$$

where S is a solution of the following Riccati Algebraic Equation.

$$\begin{bmatrix} A & 0 \\ -C & 0 \end{bmatrix}^T S + S\begin{bmatrix} A & 0 \\ -C & 0 \end{bmatrix} - R^{-1}S\begin{bmatrix} B \\ 0 \end{bmatrix}\begin{bmatrix} B \\ 0 \end{bmatrix}^T S = -Q \quad (37)$$

As mentioned above, the feedback controller gain K_1 and K_2 are computed.

$$[\,K_1 \ K_2\,] = R^{-1}\begin{bmatrix} B \\ 0 \end{bmatrix}^T S \ , \quad (38)$$

where K_1 and K_2 are the gain of the feedback controller. This extended system is a decoupling system in which the X-direction and Y-direction do not interfere. Then, the X-direction and Y-direction were considered independently, and a feedback control system was built for each direction. Moreover, since this extended system was set to be constant in rope length, a gain-scheduled control was applied for the change of rope length, and then the robustness of the control system was increased. The obtained weighting matrix of Q is shown as follows:

$$Q = [\,10^2 \ 10^2 \ 10^3 \ 10^2 \ 10^2\,] \quad (39)$$

Next, the feedback controller of the Z-direction was built. In the Z-direction, it was assumed that stationary disturbance such as wind does not require consideration. Therefore, a feedback controller by the optimal regulator system was built. From Eq.(15), the state equation by the load position of the Z-direction is as follows.

$$\frac{d}{dt}\begin{bmatrix} z_e \\ \dot{z}_e \end{bmatrix} = \begin{bmatrix} 0 & 1 \\ 0 & 0 \end{bmatrix}\begin{bmatrix} z_e \\ \dot{z}_e \end{bmatrix} + \begin{bmatrix} 0 \\ 1 \end{bmatrix}u_l \quad (40)$$

From Eq.(40), the cost function by the load position of Z-direction is as follows.

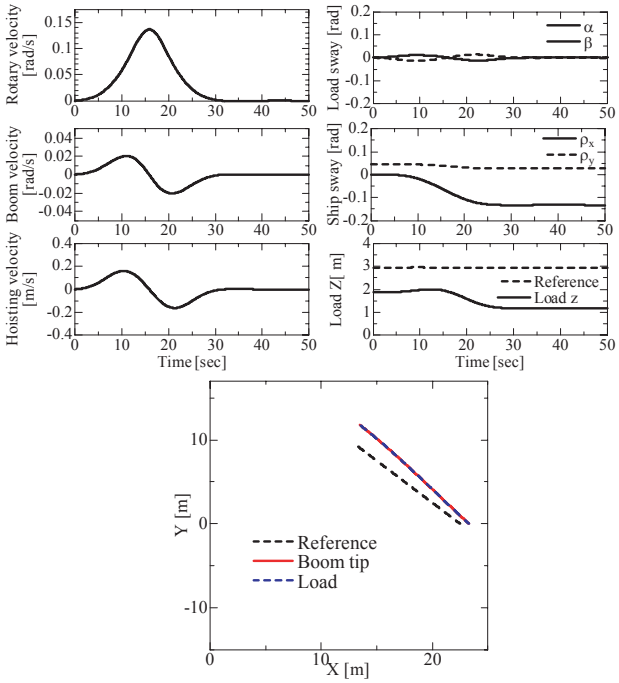

Fig. 8. Simulation results of the straight transfer with the FF control

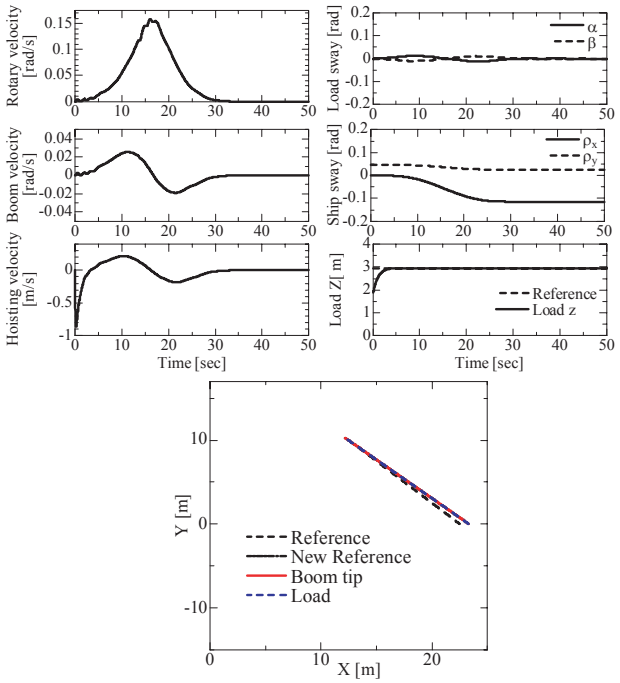

Fig. 9. Simulation results of the Two-degree-of-freedom system

$$J_z = \int_0^\infty \left\{ \begin{bmatrix} z_e \\ \dot{z}_e \end{bmatrix}^T Q_z \begin{bmatrix} z_e \\ \dot{z}_e \end{bmatrix} + R_z u_{ez}^2 \right\} \tag{41}$$

$$Q_z = [\, q_{z1} \;\; q_{z2} \,], \quad R_z = 1$$

Here Q_z and R_z are the weighting matrices for the cost function. Feedback controller gain was computed from the Riccati algebraic equation, similar to the X and Y directions. As described above, a feedback system for three-dimensional transfer trajectory control was established, and the obtained weighting matrix of Q_z is as follows:

$$Q_z \left[\, 10^3 \;\; 10^2 \, \right] \tag{42}$$

5. TRANSFER SIMULATION

A transfer control simulation by the proposed 2-DOF control system was performed. Moreover, rotary transfer without control, and feedforward control by combining the STT controller and feedforward controller was also studied by simulation analysis. The simulation was performed using the shipboard crane model. The simulation result by feedforward transfer is shown in Fig. 8 and the 2-DOF control system is shown in Fig. 9, where, in the X-Y plane, $Reference$ is P as input to the $FFcontroller$ shown in Fig. 6. $New\ Reference$ is the trajectory reference calculated by using u_{FF} and the initial state in Fig. 6, where the calculation method is omitted due to the paper limitation.

In the rotary transfer, which does not conduct sway control, a load sways outside the $Reference$ trajectory under the influence of centrifugal force and therefore the ship inclination, as shown in Fig. 4. Then, in transfer, the feedforward control which combines the STT method with the FSA method can be successfully applied to eliminate load sway and ship sway, as shown in Fig. 8. Furthermore, against disturbance like an initial error, it was confirmed that it could transfer a load to a target position using a 2-DOF control system, as shown in Fig. 9.

An evaluative comparison of the STT control, the feedforward control, and the 2-DOF control were performed. Let the transfer time be the time when the transfer end point was settled within ±0.05 [m] about each axial direction. Let the control input time be the time when the velocity inputs of both the rotary angle and boom luffing angle were settled within ±0.01 [rad/s]. Each simulation result is shown in Table 4.

Table 4. Simulation results of shipboard crane

	non control	FF control	2-DOF control
maximum sway of load [rad]	0.1616	0.0144	0.0107
control input time [sec]	15.18	27.08	27.84
transfer time [sec]	non	non	30.34

When the sway suppression controller proposed by this research is used, it was confirmed that load sway is suppressed by the feedforward control and 2-DOF control. It is considered that the sway control of the ship was effective in addition to the load sway control. The stabilization times of the control input were compared. The time of a noncontrol system using the conventional trapezoidal velocity input is 15.18[sec]. On the other hand, the time of feedforward control is 27.08 [sec], with a delay of 11.9[sec] compared with the noncontrol. This is the delay by the sway suppression controller. Also, the time of the 2-DOF control is almost the same as that of the feedforward control. In comparing the transfer time to the target position, neither the noncontrol nor the feedforward control could arrive at the target position.

As mentioned above, when cost and sway suppression

control are considered, feedforward control is desirable, but transfer to the target position is difficult only for the feedforward control. For this reason, it is thought that transfer control by 2-DOF control is more effective.

6. CONCLUSION

The following results were obtained by this research.

- A shipboard crane was modeled.
- A feedforward controller was presented by combining the frequency shape approach method with the straight transfer transformation method.
- It was confirmed that the sway of the load and the ship using the feedforward controller were reduced.
- To compensate for disturbance, a 2-DOF control system was proposed combining a feedforward control system with a feedback control system that was built using the optimal regulator.
- Three-dimensional trajectory control of the shipboard crane was performed using the 2-DOF control system, and its effectiveness was demonstrated.

In the future, the validity of the shipboard crane model will be verified by experiments or Fluid Computational Simulation (Commercial software: Flow-3D).

REFERENCES

M.D. Todd, S.T. Vohra, and F. Leban ; Dynamical Measurements of Ship Crane Load Pendulation, OCEANS '97. MTS/IEEE Conference Proceedings, Vol.2, pp.1230-1236, 1997.

B. Wen, A. Homaifar, and M. Bikdash, B. Kimiaghalam ; Modeling and Optimal Control Design of Shipboard Crane, Proceedings of American Control Conference, Vol.1999, No.Vol.1, pp.593-597, 1999.

B. Kimiaghalam, A. Homaifar, and M. Bikdash ; Pendleton Suppression of A Shipboard Crane Using Fuzzy Controller, Proceedings of American Control Conference, Vol.1999, No.Vol.1, pp.586-590, 1999.

C. Chin, A.H. Nayfeh, and D.T. Mook ; Dynamics And Control of Ship-Mounted Cranes, Collect Tech Pap, Vol.39th, No.Pt.1, pp.295-301, 1998.

A. Tsutsu, and M. Uejima ; Vertical Lifting Control for A Floating Crane, 7th SICE System and Integration Symposium (SI2006), pp.842-843, 2006.

Y. Shen, K. Terashima, and K. Yano ; Optimal Control of Rotary Crane Using The Straight Transfer Transformation Method to Eliminate Residual Vibration, Trans. of the Society of Instrument and Control Engineers, Vol.39, No.9, pp.817-826, 2003.

K. Terashima, Y. Shen, and K. Yano ; Modeling And Optimal Control of A Rotary Crane Using The Straight Transfer Transformation Method, Int. J. of Control Engineering Practice 15, Elsevier, pp.1179-1192, 2007.

K. Yano, T. Toda, and K. Terashima ; Sloshing Suppression Control of Automatic Pouring Robot by Hybrid Shape Approach, Proc. of IEEE CDC, Floria, Sept, pp.1328-1333, 2001.

Appendix A. DERIVATION OF EQS.(1) AND (2) FOR CRANE MODEL

A crane tip is assumed to be a cart which moves in the X, Y, and Z-direction as shown in Fig. 3. The load position expressed by the swing angle (α, β) is shown as follows:

$$x' = \tilde{x}' + \frac{l\sin\alpha\cos\beta}{\sqrt{1-\sin^2\alpha\sin^2\beta}} \tag{A.1}$$

$$y' = \tilde{y}' + \frac{l\cos\alpha\sin\beta}{\sqrt{1-\sin^2\alpha\sin^2\beta}} \tag{A.2}$$

$$z' = \tilde{z}' - \frac{l\cos\alpha\cos\beta}{\sqrt{1-\sin^2\alpha\sin^2\beta}} \tag{A.3}$$

Since it will be $\sin^2\alpha\sin^2\beta \cong 0$, if α and β are minimal, on approximation:

$$\sin^2\alpha\sin^2\beta = 0 \tag{A.4}$$

Eqs.(A.1)$\sim$(A.3) become

$$x' = \tilde{x}' + l\sin\alpha\cos\beta \tag{A.5}$$

$$y' = \tilde{y}' + l\cos\alpha\sin\beta \tag{A.6}$$

$$z' = \tilde{z}' - l\cos\alpha\cos\beta \tag{A.7}$$

Where, it is the Lagrange equation,

$$\frac{d}{dt}\left(\frac{\partial T}{\partial \dot{q}}\right) - \frac{\partial T}{\partial q} + \frac{\partial U}{\partial q} = 0 \tag{A.8}$$

$$T = T_x + T_y + T_z \tag{A.9}$$

$$T_{x'} = \frac{1}{2}M\dot{\tilde{x}}'^2 + \frac{1}{2}m\left\{\frac{d}{dt}\left(\tilde{x}' + l\sin\alpha\cos\beta\right)\right\}^2 \tag{A.10}$$

$$T_{y'} = \frac{1}{2}M\dot{\tilde{y}}'^2 + \frac{1}{2}m\left\{\frac{d}{dt}\left(\tilde{y}' + l\cos\alpha\sin\beta\right)\right\}^2 \tag{A.11}$$

$$T_{z'} = \frac{1}{2}M\dot{\tilde{z}}'^2 + \frac{1}{2}m\left\{\frac{d}{dt}\left(\tilde{z}' - l\cos\alpha\cos\beta\right)\right\}^2 \tag{A.12}$$

$$U = Mg\tilde{z}' + mg\left(z' - l\cos\alpha\cos\beta\right) \tag{A.13}$$

Where the solution about the swing angle is shown as follows:

$$\ddot{\theta} = u_\theta, \quad \ddot{\phi} = u_\phi, \quad \ddot{l} = u_l$$

$$\ddot{\alpha} = -\frac{\left(\dot{\alpha}^2+\dot{\beta}^2\right)B + \dddot{\tilde{x}}'C + \dddot{\tilde{y}}'D + \left(g+\dddot{\tilde{z}}'\right)E + \dot{\alpha}\dot{\beta}F}{A}\cdots$$
$$\cdots \underline{+\ddot{l}G + \dot{\alpha}\dot{l}H} \tag{A.14}$$

$$\ddot{\beta} = -\frac{\left(\dot{\alpha}^2+\dot{\beta}^2\right)I + \dddot{\tilde{x}}'J + \dddot{\tilde{y}}'K + \left(g+\dddot{\tilde{z}}'\right)L + \dot{\alpha}\dot{\beta}M}{A}\cdots$$
$$\cdots \underline{+\ddot{l}N + \dot{\beta}\dot{l}H} \tag{A.15}$$

However

$$\dddot{\tilde{x}}' = -L_B\{\ddot{\phi}\sin\phi\cos\theta + (\dot{\phi}^2+\dot{\theta}^2)\cos\phi\cos\theta$$
$$-2\dot{\phi}\dot{\theta}\sin\phi\sin\theta + \ddot{\theta}\cos\phi\sin\theta\},$$

$$
\begin{aligned}
\ddot{\tilde{y}}' &= -L_B\{\ddot{\phi}\sin\phi\sin\theta + (\dot{\phi}^2+\dot{\theta}^2)\cos\phi\sin\theta \\
&\quad +2\dot{\phi}\dot{\theta}\sin\phi\cos\theta - \ddot{\theta}\cos\phi\cos\theta\}, \\
\ddot{\tilde{z}}' &= L_B(\ddot{\phi}\cos\phi - \dot{\phi}^2\sin\phi), \\
e_x &= x' - \tilde{x}', \quad e_y = y' - \tilde{y}', \quad e_z = z' - \tilde{z}', \\
A &= \sin^2\alpha\sin^2\beta + \cos^2\alpha\cos^2\beta, \quad B = \cos\alpha\sin\alpha\sin^2\beta, \\
C &= \cos^3\alpha\cos\beta/l, \quad D = -\sin\alpha\sin^3\beta/l, \\
E &= \sin\alpha\cos\beta\left(\sin^2\beta + \cos^2\alpha\right)/l, \\
F &= -2\cos^2\alpha\sin\beta\cos\beta, \quad G = -\cos\alpha\sin\alpha\sin^2\beta/l, \\
H &= 2A/l, \quad I = \sin^2\alpha\cos\beta\sin\beta, \quad J = -\sin^3\alpha\sin\beta/l, \\
K &= \cos\alpha\cos^3\beta/l, \quad L = \cos\alpha\sin\beta\left(\sin^2\alpha + \cos^2\beta\right)/l, \\
M &= -2\cos\alpha\sin\alpha\cos^2\beta, \quad N = \sin^2\alpha\sin\beta\cos\beta/l
\end{aligned}
$$

Here u_θ, u_ϕ, and u_l are inputs of the rotary crane.

Eqs.(1) and (2) are shown in the text.

Appendix B. DERIVATION OF EQS.(6)∼(8) FOR CRANE MODEL

The ship's rotational motion is expressed by rolling, pitching and yawing, but in this paper, the yawing angle is not taken into consideration and is assumed to be $\rho_z = 0$. The rotation matrix of each axis is shown in Eqs.(B.1) and (B.2).

$$
R(x,\rho_x) = \begin{bmatrix} 1 & 0 & 0 \\ 0 & \cos\rho_x & -\sin\rho_x \\ 0 & \sin\rho_x & \cos\rho_x \end{bmatrix} \tag{B.1}
$$

$$
R(y,\rho_y) = \begin{bmatrix} \cos\rho_y & 0 & \sin\rho_y \\ 0 & 1 & 0 \\ -\sin\rho_y & 0 & \cos\rho_y \end{bmatrix} \tag{B.2}
$$

As a result, The rotation matrix R_{xy} can be given by Eq.(B.3).

$$
\begin{aligned}
R_{xy} &= R(y,\rho_y)\,R(x,\rho_x) \\
&= \begin{bmatrix} \cos\rho_y & \sin\rho_y\sin\rho_x & \sin\rho_y\cos\rho_x \\ 0 & \cos\rho_x & -\sin\rho_x \\ -\sin\rho_y & \cos\rho_y\sin\rho_x & \cos\rho_y\cos\rho_x \end{bmatrix}
\end{aligned} \tag{B.3}
$$

Next, the translational matrix from the ship center to the rotary crane is shown in Eq.(B.4).

$$
p = \begin{bmatrix} D_l\cos\rho_y \\ 0 \\ -D_l\sin\rho_y \end{bmatrix} \tag{B.4}
$$

Eqs.(B.3) and (B.4) are used to create a matrix to translate coordinates from the crane coordinate system to the absolute coordinate system as follows:

$$
\begin{aligned}
T &= \left[\begin{array}{c|c} R_{xy} & p \\ \hline 0 & 1 \end{array}\right] \\
&= \begin{bmatrix} \cos\rho_y & \sin\rho_y\sin\rho_x & \sin\rho_y\cos\rho_x & D_l\cos\rho_y \\ 0 & \cos\rho_x & -\sin\rho_x & 0 \\ -\sin\rho_y & \cos\rho_y\sin\rho_x & \cos\rho_y\cos\rho_x & -D_l\sin\rho_y \\ 0 & 0 & 0 & 1 \end{bmatrix}
\end{aligned} \tag{B.5}
$$

When Eq.(B.5) is used, the crane tip position in the absolute coordinate system is as follows:

$$
\tilde{X}_B = T\tilde{X}'_B\ , \tag{B.6}
$$

where

$$
\tilde{X}_B = \left[\,\tilde{x}\ \tilde{y}\ \tilde{z}\ 1\,\right]^T, \qquad \tilde{X}'_B = \left[\,\tilde{x}'\ \tilde{y}'\ \tilde{z}'\ 1\,\right]^T
$$

Moreover, the load position in the absolute coordinate system,

$$
x = \tilde{x} + l\sin\alpha\cos\beta \tag{B.7}
$$

$$
y = \tilde{y} + l\cos\alpha\sin\beta \tag{B.8}
$$

$$
z = \tilde{z} - l\cos\alpha\cos\beta\ , \tag{B.9}
$$

where $\ddot{\tilde{x}}$, $\ddot{\tilde{y}}$, $\ddot{\tilde{z}}$ are

$$
\frac{d\tilde{X}_B}{dt} = \frac{dT}{dt}\tilde{X}_B + T\frac{d\tilde{X}'_B}{dt} \tag{B.10}
$$

$$
\frac{d}{dt}\left(\frac{d\tilde{X}_B}{dt}\right) = \frac{d}{dt}\left(\frac{dT}{dt}\right)\tilde{X}'_B + 2\frac{dT}{dt}\frac{d\tilde{X}'_B}{dt} + T\frac{d}{dt}\left(\frac{d\tilde{X}'_B}{dt}\right) \tag{B.11}
$$

$$
\begin{aligned}
\ddot{\tilde{x}} &= \cos\rho_y\ddot{\tilde{x}}' + \sin\rho_y\sin\rho_x\ddot{\tilde{y}}' + \sin\rho_y\cos\rho_x\ddot{\tilde{z}}' \\
&\quad -2\dot{\rho_y}\sin\rho_y\dot{\tilde{x}}' + 2\left(\dot{\rho_y}\cos\rho_y\sin\rho_x + \dot{\rho_x}\sin\rho_y\cos\rho_x\right)\dot{\tilde{y}}' \\
&\quad +2\left(\dot{\rho_y}\cos\rho_y\cos\rho_x - \dot{\rho_x}\sin\rho_y\sin\rho_x\right)\dot{\tilde{z}}' \\
&\quad -\left(\ddot{\rho_y}\sin\rho_y + {\dot{\rho_y}}^2\cos\rho_y\right)\tilde{x}' \\
&\quad +\{\ddot{\rho_y}\cos\rho_y\sin\rho_x + \ddot{\rho_x}\sin\rho_y\cos\rho_x \\
&\quad -\left({\dot{\rho_y}}^2 + {\dot{\rho_x}}^2\right)\sin\rho_y\sin\rho_x + 2\dot{\rho_y}\dot{\rho_x}\cos\rho_y\cos\rho_x\}\,\tilde{y}' \\
&\quad +\{\ddot{\rho_y}\cos\rho_y\cos\rho_x - \ddot{\rho_x}\sin\rho_y\sin\rho_x \\
&\quad -\left({\dot{\rho_y}}^2 + {\dot{\rho_x}}^2\right)\sin\rho_y\cos\rho_x - 2\dot{\rho_y}\dot{\rho_x}\cos\rho_y\sin\rho_x\}\,\tilde{z} \\
&\quad -D_l\left(\ddot{\rho_y}\sin\rho_y + {\dot{\rho_y}}^2\cos\rho_y\right)
\end{aligned} \tag{B.12}
$$

$$
\begin{aligned}
\ddot{\tilde{y}} &= \cos\rho_x\ddot{\tilde{y}}' - 2\dot{\rho_x}\sin\rho_x\dot{\tilde{y}}' - \left(\ddot{\rho_x}\sin\rho_x + {\dot{\rho_x}}^2\cos\rho_x\right)\tilde{y}' \\
&\quad +\sin\rho_x\ddot{\tilde{z}}' + 2\dot{\rho_x}\cos\rho_x\dot{\tilde{z}}' + \left(\ddot{\rho_x}\cos\rho_x - {\dot{\rho_x}}^2\sin\rho_x\right)\tilde{z}'
\end{aligned} \tag{B.13}
$$

$$
\begin{aligned}
\ddot{\tilde{z}} &= -\sin\rho_y\ddot{\tilde{x}}' + \cos\rho_y\sin\rho_x\ddot{\tilde{y}}' + \cos\rho_y\cos\rho_x\ddot{\tilde{z}}' \\
&\quad -2\dot{\rho_y}\cos\rho_y\dot{\tilde{x}}' + \left(-\ddot{\rho_y}\cos\rho_y + {\dot{\rho_y}}^2\sin\rho_y\right)\tilde{x}' \\
&\quad +2\left(-\dot{\rho_y}\sin\rho_y\sin\rho_x + \dot{\rho_x}\cos\rho_y\cos\rho_x\right)\dot{\tilde{y}}' \\
&\quad +\{-\ddot{\rho_y}\sin\rho_y\sin\rho_x + \ddot{\rho_x}\cos\rho_y\cos\rho_x \\
&\quad -\left({\dot{\rho_y}}^2 + {\dot{\rho_x}}^2\right)\cos\rho_y\sin\rho_x - 2\dot{\rho_y}\dot{\rho_x}\sin\rho_y\cos\rho_x\}\,\tilde{y}' \\
&\quad -2\left(\dot{\rho_y}\sin\rho_y\cos\rho_x + \dot{\rho_x}\cos\rho_y\sin\rho_x\right)\dot{\tilde{z}}' \\
&\quad +\{-\ddot{\rho_y}\sin\rho_y\cos\rho_x - \ddot{\rho_x}\cos\rho_y\sin\rho_x \\
&\quad -\left({\dot{\rho_y}}^2 + {\dot{\rho_x}}^2\right)\cos\rho_y\cos\rho_x + 2\dot{\rho_y}\dot{\rho_x}\sin\rho_y\sin\rho_x\}\,\tilde{z}' \\
&\quad -D_l\left(\ddot{\rho_y}\cos\rho_y - {\dot{\rho_y}}^2\sin\rho_y\right)
\end{aligned} \tag{B.14}
$$

Eqs.(6)∼(8) are shown in the text.